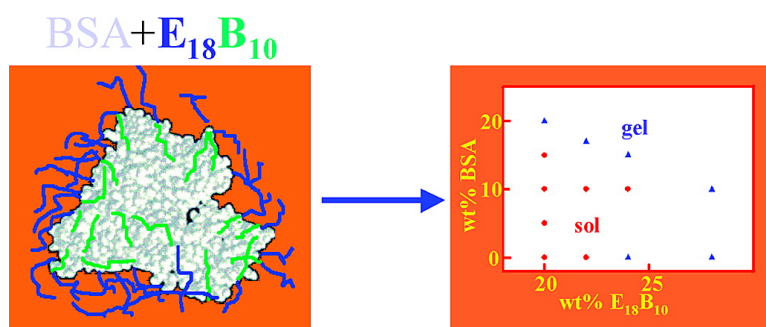


## Interactions of Bovine Serum Albumin with Ethylene Oxide/Butylene Oxide Copolymers in Aqueous Solution

Antonios Kellarakis, Valeria Castelletto, Marta J. Krysmann,  
Vasiliki Havredaki, Kyriakos Viras, and Ian W. Hamley

*Biomacromolecules*, 2008, 9 (5), 1366-1371 • DOI: 10.1021/bm800046m • Publication Date (Web): 08 April 2008

Downloaded from <http://pubs.acs.org> on January 8, 2009



### More About This Article

Additional resources and features associated with this article are available within the HTML version:

- Supporting Information
- Access to high resolution figures
- Links to articles and content related to this article
- Copyright permission to reproduce figures and/or text from this article

[View the Full Text HTML](#)



# Articles

## Interactions of Bovine Serum Albumin with Ethylene Oxide/Butylene Oxide Copolymers in Aqueous Solution

Antonios Kelarakis,<sup>\*,†</sup> Valeria Castelletto,<sup>‡</sup> Marta J. Krysmann,<sup>‡</sup> Vasiliki Havredaki,<sup>†</sup> Kyriakos Viras,<sup>†</sup> and Ian W. Hamley<sup>\*,‡</sup>

National and Kapodistrian University of Athens, Department of Chemistry, Physical Chemistry Laboratory, Panepistimiopolis, 157 71 Athens, Greece, and School of Chemistry, The University of Reading, Post Office Box 224, Whiteknights, Reading RG6 6AD, United Kingdom

Received January 15, 2008; Revised Manuscript Received February 12, 2008

The interactions of bovine serum albumin (BSA) with three ethylene oxide/butylene oxide (E/B) copolymers having different block lengths and varying molecular architectures is examined in this study in aqueous solutions. Dynamic light scattering (DLS) indicates the absence of BSA–polymer binding in micellar systems of copolymers with lengthy hydrophilic blocks. On the contrary, stable protein–polymer aggregates were observed in the case of E<sub>18</sub>B<sub>10</sub> block copolymer. Results from DLS and SAXS suggest the dissociation of E/B copolymer micelles in the presence of protein and the absorption of polymer chains to BSA surface. At high protein loadings, bound BSA adopts a more compact conformation in solution. The secondary structure of the protein remains essentially unaffected even at high polymer concentrations. Raman spectroscopy was used to give insight to the configurations of the bound molecules in concentrated solutions. In the vicinity of the critical gel concentration of E<sub>18</sub>B<sub>10</sub> introduction of BSA can dramatically modify the phase diagram, inducing a gel–sol–gel transition. The overall picture of the interaction diagram of the E<sub>18</sub>B<sub>10</sub>–BSA reflects the shrinkage of the suspended particles due to destabilization of micelles induced by BSA and the gelator nature of the globular protein. SAXS and rheology were used to further characterize the structure and flow behavior of the polymer–protein hybrid gels and sols.

### 1. Introduction

The interactions between proteins and macromolecules bearing poly(ethylene oxide) (PEO) segments have attracted much attention from both academia and industry, not least because PEO is a FDA (United States Food and Drug Administration)-approved polymer for medical uses due to its nontoxic, biodegradable, and cell-compatible characteristics.<sup>1–3</sup> Specific interest for PEO lies on the development of synthetic systems for biomedical applications such as antifouling technology (prevention of Biofilm formation),<sup>4</sup> tissue engineering, and artificial organs.<sup>5</sup>

The main body of PEO–protein investigations centers on PEO brush-coated surfaces; an analytical presentation of the progress achieved in this field is given in ref 6 together with the corresponding theoretical models. It is well-established that PEO brush-coated surfaces can suppress protein absorption,<sup>7</sup> enabling longer in vivo half-lives of coated surfaces. This behavior has been assigned to the high degree of PEO hydration that imposes steric constraints to the diffusive motion of proteins by setting a high activation energy for the protein to penetrate the brush.<sup>8</sup> Other factors contributing to protein repellency from PEO are electrostatic double layers forces, hydrodynamic lubrication forces, and enthalpic penalties due to disruption of hydrogen bridges with water.<sup>9</sup>

At the same time, it has been supported that the inert character of PEO against BSA deposition is weakened in the case of low-density grafted surfaces,<sup>10</sup> at high protein loads,<sup>11</sup> for low PEO molar mass, or by compression of the brush.<sup>11</sup> PEO–protein attractive interactions have been recognized, including hydrogen bridging and electrostatic and van der Waals forces (such as hydrophobic interactions).<sup>9</sup> Moreover, an increasing number of studies indicate the development of PEO–protein complexes in aqueous media. For example, complexes have been reported for PEO with pepsin,<sup>12</sup> lysozyme,<sup>13</sup> serum albumin,<sup>14,15</sup> and alpha-chymotrypsin.<sup>16</sup> Interactions between protein and PEO conjugates have also been investigated; recently, the binding mechanism between BSA and a polyethylene glycol lipid has been monitored,<sup>17,18</sup> evidence of complexation between ethylene oxide/propylene oxide and alpha-chymotrypsin was reported,<sup>19</sup> while a later study indicates that no complexation was detected either between E/P copolymers (P-polypropylene oxide) and BSA or between E/P and lysozyme.<sup>20</sup>

In this report we extend the field of investigations of BSA–ethylene oxide-based copolymers by considering a series of ethylene oxide/butylene oxide (E/B) copolymers having a variety of hydrophilic and hydrophobic block lengths and different molecular architecture. E/B copolymers represent a well-studied class of macromolecular surface-active agents that micellize in water, with the micellar core dominated by the B block, while E groups are extended in the solvent.<sup>21,22</sup> Serum albumin is the dominant protein of blood plasma that has been widely studied<sup>23</sup> and is now produced in industrial scale.

\* To whom correspondence should be addressed. E-mail: akelar@cc.uoa.gr (A.K.); i.w.hamley@reading.ac.uk (I.W.H.).

<sup>†</sup> National and Kapodistrian University of Athens.

<sup>‡</sup> The University of Reading.

**Table 1.** Molecular Characteristics of the Copolymers<sup>a</sup>

copolymer	$M_n/g \cdot mol^{-1}$	wt. % E	$M_w/M_n$
E <sub>18</sub> B <sub>10</sub>	1510	52	1.04
B <sub>20</sub> E <sub>430</sub>	20400	92.9	1.06
B <sub>20</sub> E <sub>610</sub>	28300	95	1.09

<sup>a</sup> Estimated uncertainty:  $M_n$  to  $\pm 5\%$ ; wt. % E to  $\pm 1$ ;  $M_w/M_n$  to  $\pm 0.01$ .

Within the background of conflicting reports concerning complexation presented above, the aim of this study is to explore the possible patterns of interactions between PEO-based copolymers and BSA and examine the strength of the copolymer–protein interaction with respect to the block length of the polymer. The dimensions and structure of polymer–protein interactions in buffer solution pH = 7.4 were monitored by dynamic light scattering (DLS) and small-angle X-ray scattering (SAXS), respectively. Information about the secondary structure of BSA in hybrid systems was obtained from circular dichroism (CD). Raman spectroscopy was used to monitor conformation changes induced by BSA in concentrated hybrid systems. The polymer–protein interaction diagram was drawn and the protein-induced changes in crystalline structure and viscoelastic response of polymer gels were investigated by SAXS and linear viscoelasticity.

## 2. Experimental Section

**2.1. Materials.** BSA ( $M_w = 66000$  g/mol) and phosphate buffer saline (PBS, pH 7.4, ionic strength  $I = 0.169$  M) were obtained from Sigma. E<sub>18</sub>B<sub>10</sub><sup>24–26</sup> (code BM45-1600; also denoted E<sub>18</sub>B<sub>9</sub>,<sup>27–29</sup> EB 18-9<sup>29,30</sup> in other studies) was obtained from Dow Chemical Co. The preparation of copolymers B<sub>20</sub>E<sub>430</sub> and B<sub>20</sub>E<sub>620</sub> was by sequential anionic polymerization of BO followed by EO (we denote the polymers so produced as B<sub>m</sub>E<sub>n</sub> to signify the change in the copolymerization route), as described previously.<sup>31</sup> For all polymers considered, Gel permeation chromatography (GPC) was used to confirm narrow chain length distributions, and <sup>13</sup>C NMR spectroscopy was used to obtain absolute values of number-average molar mass. The molecular characteristics of the copolymers are summarized in Table 1.

Copolymers were first dissolved in PBS by vigorous mixing for 1 h and then stored at room temperature for a day. BSA was then added to the polymer solutions and the hybrid systems were stirred for 2 h. For concentrated samples, both components were dissolved simultaneously in the buffer solvent through stirring for 24 h.

**2.2. Methods.** *Dynamic Light Scattering (DLS).* Dynamic light scattering (DLS) measurements were carried out on well-filtered solutions by means of an ALV/CGS-3 Compact Goniometer System with ALV/LSE-5003 correlator using vertically polarized incident light of wavelength  $\lambda = 632.8$  nm. Measurements were performed at angle  $\theta = 90^\circ$  to the incident beam and data were collected three times for 30 s. The intensity autocorrelation functions were analyzed by the constrained regularized CONTIN method<sup>32</sup> to obtain distributions of decay rates ( $\Gamma$ ), hence, distributions of apparent mutual diffusion coefficient  $D_{app} = \Gamma/q^2$  [ $q = (4\pi n/\lambda)\sin(\theta/2)$ , where  $n$  is the refractive index of the solvent and  $\theta$  is the scattering angle], and ultimately of apparent hydrodynamic radius of the particle via the Stokes–Einstein equation

$$r_h = k_B T / (6\pi\eta D_{app}) \quad (1)$$

where  $k_B$  is the Boltzmann constant and  $\eta$  is the viscosity of the solvent at temperature  $T$ .

*Small Angle X-ray Scattering (SAXS).* SAXS experiments were performed on beamline 2.1, Synchrotron Radiation Source, Daresbury, U.K. The wavelength of synchrotron radiation was 1.5 Å and the sample-to-detector distance was 3 m. Samples were mounted between mica windows in a liquid cell with water-bath temperature control. Two-

dimensional SAXS patterns were collected using a RAPID area detector. All patterns were corrected for the incident beam fluctuations as well as air and instrument scattering. The SAXS  $q$  scale ( $q = 4\pi\sin\theta/\lambda$ , where  $2\theta$  is the scattering angle) was calibrated by using rat tendon collagen standards. 2D SAXS patterns were converted into 1D profiles using BSL software.

*Rheology.* Rheological properties were determined using a controlled stress TA Instruments AR-2000 rheometer (TA Instruments). A cone-and-plate geometry (cone diameter 20 mm, angle  $1^\circ$ ) was used for all samples. Frequency scans were performed within the angular frequency range ( $\omega$ ) 0.5–600 rad/sec, with the instrument in oscillatory mode at 25 °C. Preliminary strain sweeps were performed for each sample to define the linear viscoelastic region, thus ensuring that moduli were independent of strain.

*Circular Dichroism.* The circular dichroism (CD) spectra were recorded on a Chirascan spectropolarimeter (Applied Photophysics, U.K.). A quartz coverslip cuvette with 0.1 mm path length was used. The BSA samples (0.1 wt % BSA) were mixed with varying amounts of copolymers and incubated for 1 h before testing. Spectra were obtained from 190 to 250 nm with a 0.5 nm step, 1 nm bandwidth, and 1 s collection time per step at 20 °C, taking five averages. Spectra were corrected against background.

*Raman Spectroscopy.* Raman spectra of concentrated samples were recorded by a Perkin-Elmer GX Fourier transform spectrometer, equipped with an excitation source of a diode pumped Nd:YAG laser at 1064  $cm^{-1}$ . The laser power was set at 500 mW and the resolution was 4  $cm^{-1}$ . Spectra were monitored from 3500 to 500  $cm^{-1}$  with interval 2  $cm^{-1}$  and analyzed using GRAMS/32 data analysis software.

## 3. Results and Discussion

### 3.1. Polymer–Protein Interactions in Dilute Solutions.

Intensity fraction distributions of apparent hydrodynamic radius ( $r_h$ ) of solutions containing 1 wt % B<sub>20</sub>E<sub>430</sub> and B<sub>20</sub>E<sub>610</sub> and various weight fractions of BSA are illustrated in Figures 1a and b, respectively. Hereafter, we use the notations  $f_{BSA}$  = weight % of BSA/weight % of polymer and  $f_{polymer}$  = weight % of polymer/weight % of BSA. In Figure 1, it can be seen that the hydrodynamic radius of 1 wt % BSA buffer solution was  $r_h = 3.9$  nm in agreement with values reported in the literature.<sup>33,17</sup> The conformation of monomeric BSA was initially described<sup>34</sup> as a prolate ellipsoid with major axis 140 and minor axis 40, while later studies indicated a heart-shape structure<sup>23</sup> and recently an equilateral, triangular prismatic shell.<sup>35</sup> In Figure 1 it can also be seen that  $r_h = 24.2$  and  $r_h = 27.3$  nm for 1 wt % B<sub>20</sub>E<sub>430</sub> and B<sub>20</sub>E<sub>610</sub> buffer solution, respectively, in fair agreement with previously published values in water.<sup>31</sup> The presence of a peak at 3.9 nm in all hybrid systems presented in Figure 1 indicates the inert character of BSA toward binding with these copolymers. At the same time, the presence of peaks with  $r_h$  close to that of neat micelles, suggests that micelles of B<sub>20</sub>E<sub>430</sub> and B<sub>20</sub>E<sub>610</sub> coexist with unassociated BSA. For B<sub>20</sub>E<sub>610</sub>–BSA mixtures, besides the peaks corresponding to neat micelles and neat protein, large aggregates that grow in size with BSA weight fraction can also be observed (Figure 1b). These large aggregates may result from depletion forces induced by the long EO polymer chains in solution.<sup>36</sup>

On the other hand, the monomodal distributions observed in solutions of E<sub>18</sub>B<sub>10</sub>–BSA (Figure 2) indicate the development of stable polymer–protein aggregates. The absence of any peak corresponding to neat BSA or neat micelles suggests the action of a strong polymer–protein binding mechanism. We also note the absence of any additional peak at high  $r_h$  range, an observation that excludes the presence of any significant depletion forces in these systems. This behavior supports the

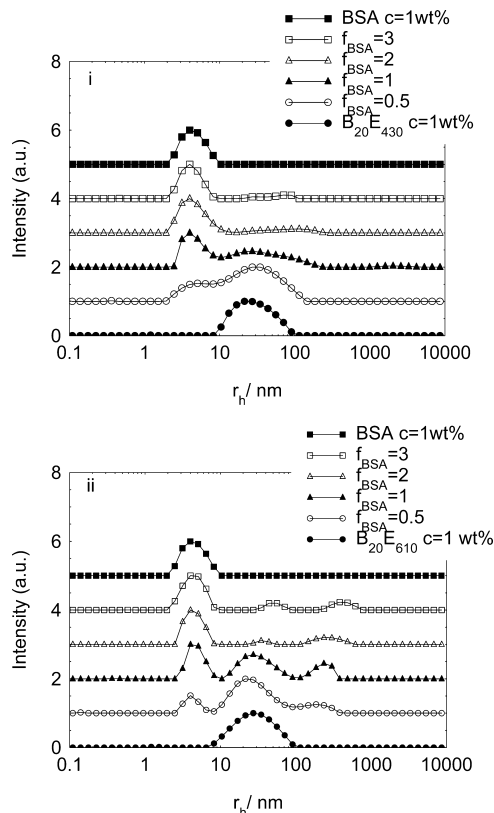


**Figure 1.** Normalized intensity fraction distributions of apparent hydrodynamic radius ( $r_h$ ) for aqueous solution of BSA mixtures with (i)  $B_{20}E_{430}$  and (ii)  $B_{20}E_{610}$  (copolymer concentration was kept constant at 1 wt %, pH = 7.4).

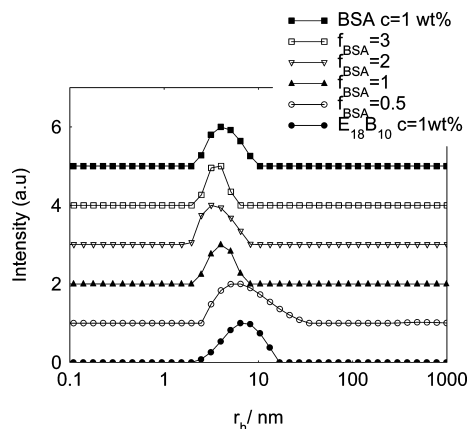


**Figure 2.** Normalized intensity fraction distributions of apparent hydrodynamic radius ( $r_h$ ) for aqueous solution of  $E_{18}B_{10}$ -BSA complexes (copolymer concentration was kept constant at 1 wt %, pH = 7.4).

disruption of micellar structure in the presence of protein, in contrast with the effects observed for E/B copolymers with lengthy hydrophilic blocks.

It seems, therefore, that the strength of the interactions developed between E/B copolymers and BSA critically depends on the size of the polymeric molecule, with short EO polymers showing a strong tendency for binding, while polymers with lengthy EO blocks appear rather inert to protein binding. It has been pointed out that the chain length of PEO is a critical parameter that dictates the absorption of proteins to PEO-grafted surfaces.<sup>37</sup>

In the particular case of  $E_{18}B_{10}$ -BSA system, a gradual decrease in  $r_h$  of the complexes was observed upon BSA

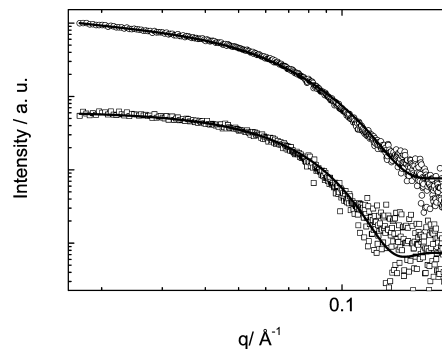


**Figure 3.** SAXS for pure BSA (circles) and  $E_{18}B_{10}$ -BSA,  $f_{BSA} = 3$  (squares). Data has been arbitrarily shifted in the y-axis to enable visualization.

addition. It seems, therefore, that the addition of BSA to aqueous solutions of  $E_{18}B_{10}$  disrupts micellization, so that copolymers do not self-associate to form micelles, but they are instead attached to the surface of the globular protein. A similar interaction mode has been established for BSA-polyethylene glycol lipid system.<sup>17,18</sup> For  $f_{BSA} = 1$  in Figure 2, one BSA molecule is covered approximately by 44 molecules of  $E_{18}B_{10}$ . At high protein loading,  $r_h$  of the complexes were found to be lower than  $r_h$  of the neat protein. This effect indicates that binding with polymer enhances the folding of the protein, that is, introduction of polymers leads to a rearrangement of the protein conformation in solution toward more compact structures. This effect was further explored by SAXS analysis.

The coherent part of the SAXS intensity from an isotropic solution of globular objects,  $I(q)$ , can be written as<sup>38</sup>

$$I(q) = kP(q)S(q) \quad (2)$$

where  $k$  is a normalization constant proportional to the number density of scatterers,  $P(q)$  is the form factor,  $S(q)$  is the structure factor, and  $q$  is the scattering vector given by  $q = 4\pi \sin\theta/\lambda$ . The systems studied in this work correspond to dilute solutions. Therefore,  $S(q) \sim 1$  in eq 1, so  $I(q)$  is proportional to the form factor  $P(q)$ .  $P(q)$  for the sample containing 1 wt % BSA, with  $f_{polymer} = 0$  and  $f_{BSA} = 3$ , was fitted to a triaxial ellipsoid with half-axis ( $a, b, c$ ):<sup>39</sup>

$$P(q) = \frac{2}{\pi} \int_0^{\pi/2} \int_0^{\pi/2} \Phi^2[q, r(a, b, c, \varphi, \theta)] \sin \varphi d\varphi d\theta \quad (3)$$

with

$$r(a, b, c, \varphi, \theta) = [(a^2 \sin^2 \theta + b^2 \cos^2 \theta) \sin^2 \varphi + c^2 \cos^2 \varphi]^{1/2} \quad (4)$$

Figure 3 shows the SAXS obtained for 1 wt % BSA solution ( $f_{polymer} = 0$ ) and polymer-BSA solution,  $f_{BSA} = 3$ . Both data could be fitted according to the model described by eqns 2–4. The parameters obtained from the fittings shown in Figure 3 correspond to  $a = 25.5 \text{ \AA}$ ,  $b = 26.9 \text{ \AA}$ , and  $c = 58 \text{ \AA}$  and  $a = 28 \text{ \AA}$ ,  $b = 28 \text{ \AA}$ , and  $c = 42 \text{ \AA}$  for  $f_{polymer} = 0$  and  $f_{BSA} = 3$ , respectively, indicating lower volume of the polymer-BSA aggregates compared to free BSA. Note that the shape of the aggregate for  $f_{polymer} = 0$  corresponds to a prolate ellipsoid, which is a particular case of eqns 3 and 4. The dimensions obtained for neat BSA are in good agreement with data previously reported in the literature.<sup>18,40,41</sup> Protein-based aggregates having lower intrinsic volume compared to the unbound particles have been reported in certain cases.<sup>42,43</sup> The effect has been assigned to pronounced dehydration of proteins due to

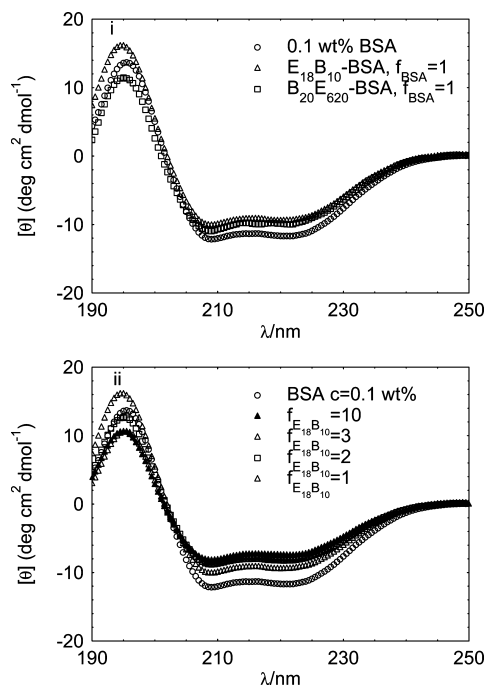


**Figure 4.** CD spectra measured for samples containing 0.1 wt % BSA and (i)  $E_{18}B_{10}$  and  $B_{20}E_{610}$ ,  $f_{BSA} = 1$ , and (ii) different fractions of added polymer  $E_{18}B_{10}$  at room temperature.

water release from the hydration layer of the protein upon complexation.

In Figure 4i, the circular dichroism (CD) spectrum of neat 0.1 wt % BSA solutions is compared with the spectra of equal concentration mixtures of BSA with  $E_{18}B_{10}$  or  $B_{20}E_{610}$ . In Figure 4ii, the comparison is made for 0.1 wt % BSA and mixtures of  $E_{18}B_{10}$ -BSA with varying polymeric content. In all cases, two distinct negative maxima at 208 and 222 nm were obtained, that are characteristic of protein having a high degree of  $\alpha$ -helical content.<sup>44,45</sup> It can be concluded that the introduction of those polymers in BSA solutions does not cause denaturation of the protein. Our observations are in agreement with several studies that conclude that certain proteins while interacting with PEO-based materials can retain their secondary structure.<sup>16,17,46-48</sup>

**3.2. Polymer-Protein Interaction in Concentrated Solutions and Gels.** Raman spectra of aqueous solutions of both E/B copolymers and BSA have been extensively studied, and the observed bands have been identified.<sup>49,50</sup> In this work we focus on the  $CH_2$  vibration mode at  $1460\text{ cm}^{-1}$  that was found to exhibit significant displacement upon protein addition in 20 wt %  $E_{18}B_{10}$  solutions. Regions of Raman spectra around  $1460\text{ cm}^{-1}$  for solutions containing 20 wt % polymer and varying amounts of added BSA are shown in Figure 5i. It can be seen that introduction of 5, 10, and 15 wt % of BSA does not affect the shape and the characteristics of the observed bands at  $1460\text{ cm}^{-1}$  region, while the peak position is shifted from  $1459\text{ cm}^{-1}$  for neat polymer solutions to  $1457\text{ cm}^{-1}$  for solutions containing 5 and 10 wt % BSA and to  $1454\text{ cm}^{-1}$  for 15 wt % BSA (Figure 5). Addition of 20 wt % BSA caused a further shift of the peak position. In other words, upon gradual addition of BSA, an initial small change in peak position is followed by a plateau region in the range 5–10 wt %, followed by a rapid decrease of peak position up to  $1450\text{ cm}^{-1}$ . We assign the plateau region in the range 5–10 wt % to systems containing densely covered BSA and the concentration region above 10 wt % to systems having lightly covered BSA. In this respect, a ratio of one BSA molecule per 88 molecules of polymer can be roughly estimated

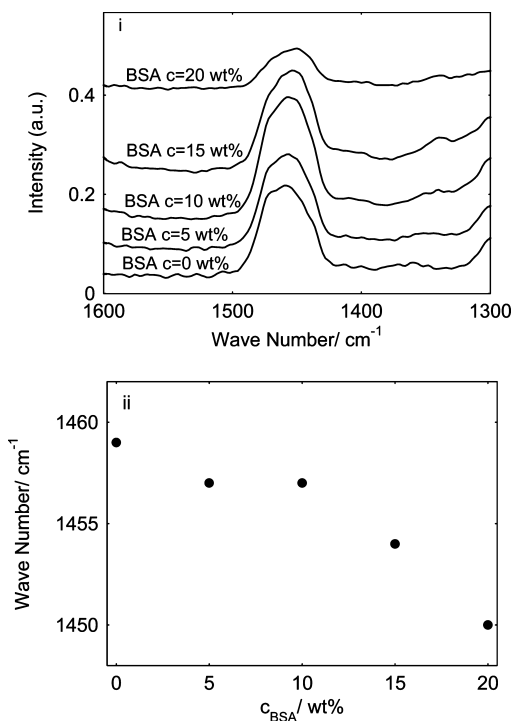


**Figure 5.** (i) Raman spectra of 20 wt %  $E_{18}B_{10}$  buffer solutions, having various amounts of added BSA. (ii) Peak position of Raman spectra corresponding to  $CH_2$  vibration mode of 20 wt %  $E_{18}B_{10}$  buffer solutions as a function of the amount of added BSA.

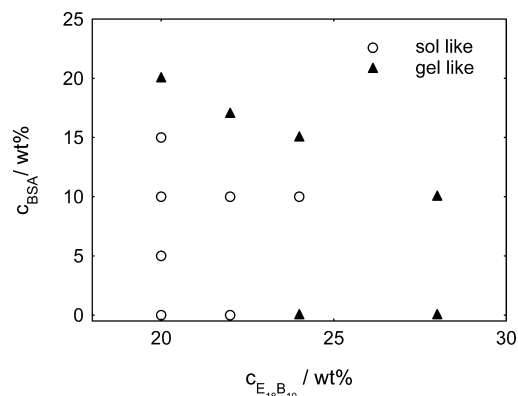


**Figure 6.** Interaction phase diagram of  $E_{18}B_{10}$ -BSA system showing selected points characterized as sol or gel solely on the basis of their fluidity.

as the saturation point of BSA. Based on  $r_h$  values of the aggregates plotted in Figure 2, the number of polymer chains to saturate one BSA molecule is significantly increased in concentrated solution compared to dilute solutions, reflecting more pronounced excluded volume effects and decreased particle mobility in the more viscous systems.

The interaction phase diagram of  $E_{18}B_{10}$ -BSA in PBS is shown in Figure 6. The diagram presented is limited between the region 20 wt % and 28 wt % of polymer content, for example, it centers around 24 wt %, which is the critical gel concentration (cgc) of the polymer. Mixtures with higher polymeric content were not considered due to the difficulty of efficient mixing of the ingredients in such viscous solutions. Mixtures with lower polymeric content were also excluded, given that the amount of BSA needed to induce phase transitions was too high, in which case, depletion effects should be also considered, complicating data interpretation. It should be noted that aqueous solutions of neat BSA exhibit a glass-like kinetic arrest at mass fractions close to 0.55.<sup>51</sup>

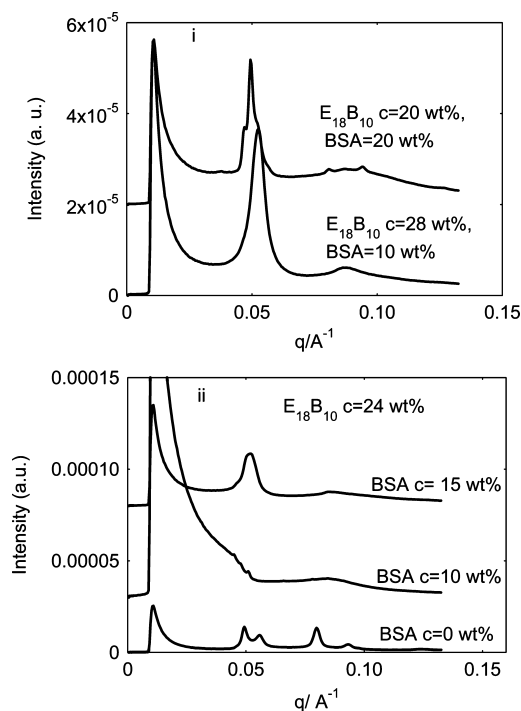


**Figure 7.** SAXS patterns of aqueous gels of  $E_{18}B_{10}$ -BSA systems at 25 °C having (i) gel-like behavior at compositions indicated and (ii) a copolymer concentration of 24 wt % and various amounts of BSA.

Selected mixtures considered in Figure 6 were characterized by SAXS, and the patterns obtained are shown in Figure 7. In Figures 6 and 7 it can be seen that BSA addition can dramatically modify the phase behavior of polymer in water. It was found that addition of 20 wt % BSA to a 20 wt %  $E_{18}B_{10}$  sol can induce a sol-to-gel transition with the resulting immobile hybrid system having a mixed structure corresponding to coexistence of fcc (dominant structure) and hexagonal packing. The domain-domain distance of that gel can be calculated from the expression  $d = 2\pi/q^*$  and was found that  $d = 127 \text{ \AA}$ . Similar trends were observed for mixtures containing 22 wt %  $E_{18}B_{10}$ . Addition of 10 wt % BSA to 24 wt %  $E_{18}B_{10}$  gel led to a gel-sol transition. This behavior directly points to strong protein-polymer binding that essentially reduces the effective volume fraction of the dispersed particles, causing the collapse of close packing. Further addition of BSA resulted in the reappearance of the gel character of the mixture. In Figure 7ii SAXS patterns that correspond to this gel-sol-gel transition (copolymer content was kept 24 wt %) are plotted. The 24 wt %  $E_{18}B_{10}$  gel showed fcc symmetry at room temperature, with  $d = 127 \text{ \AA}$ , in agreement with values reported previously.<sup>29</sup> No long-range correlation was observed for 24 wt %  $E_{18}B_{10}$ -10 wt % BSA system, but further increase in the concentration of added BSA to 15 wt % led to the evolution of a hexagonal structure with  $d = 121 \text{ \AA}$ . Gels with polymer content higher than 24 wt % retain their gel structure in the corresponding tertiary systems. A well-ordered hexagonal structure was observed for 28 wt %  $E_{18}B_{10}$ -10 wt % BSA with  $d = 119 \text{ \AA}$ , much as expected for  $E_{18}B_{10}$  gels well above the cgc.<sup>29</sup>

The phase transitions induced by BSA described above are also evident in the rheological properties of the hybrid systems, as shown in Figure 8. We note that  $G'$  of 24 wt %  $E_{18}B_{10}$  gel is reduced by 1 order of magnitude upon addition of 10 wt % BSA, consistent with the reduced viscoelasticity expected for a softer structure. Further addition of BSA resulted in enhanced

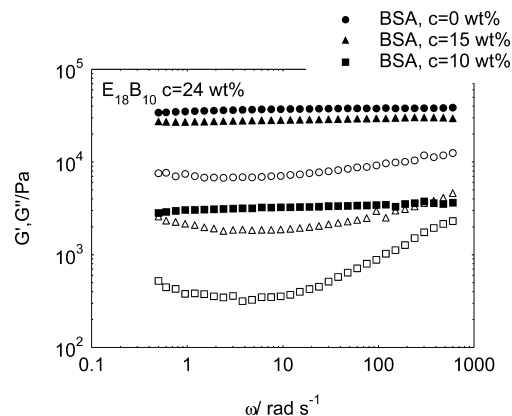


**Figure 8.** Frequency dependence of storage modulus ( $G'$ , solid symbols) and loss modulus ( $G''$ , open symbols;  $T = 25 \text{ }^\circ\text{C}$ , strain amplitude 0.5%) for  $E_{18}B_{10}$ -BSA mixtures having various amounts of added BSA with copolymer concentration 24 wt %.

viscoelasticity causing the evolution of a pseudosolid like rheological response. For this hybrid system,  $G'$  is comparable to that of neat 24 wt %  $E_{18}B_{10}$ . Therefore, the rheological response of the hybrid gels and sols can be dramatically modified depending on the amount of added BSA.

## Conclusions

In this work we report on E/B copolymer-BSA interactions in aqueous medium. The study underlines the critical role of the PEO block length to the polymer-protein binding mechanism, thus shedding some light to the contradictory literature in this field. In particular, block copolymers with lengthy PEO blocks were found not to bind with BSA in solution, preserving their micellar properties. At the same time,  $E_{18}B_{10}$  chains tend to be absorbed to the BSA surface, an effect that causes the destabilization and the collapse of copolymer micelles. The size of the dispersed particles gradually decreased upon BSA addition, while at high protein loadings, bound BSA seems to adopt a more compact structure compared to unbound BSA. The  $\alpha$ -helix content of fully bound BSA decreased slightly, although disruption of the secondary structure did not occur. Raman spectroscopy was used to provide insights into the saturation point of aggregation in concentrated solutions. Within the polymer gel phase introduction of BSA dramatically modifies both structural and rheological characteristics. The polymer-BSA interaction diagram reflects the disruption of polymer micelles induced by BSA and the resulting deswelling of dispersed particles on one hand and the gelator nature of the protein on the other. Gels close to the cgc exhibited a gel-sol-gel transition upon BSA addition and the corresponding SAXS patterns revealed, respectively, an fcc structure, a liquid-like and a poorly-ordered hexagonal system.

**Acknowledgment.** A.K. was supported by the Greek Ministry of Development-General Secretariat of Research and Technology within the 04EP36 research project.

## References and Notes

- (1) Sinha, V. R.; Aggarwal, A.; Treham, A. *Am. J. Drug Delivery* **2004**, *2*, 157.
- (2) Herold, D. A.; Keil, K.; Bruns, D. E. *Biochem. Pharmacol.* **1989**, *38*, 73.
- (3) Albertsson, P.-A. *Partition of Cell Particles and Macromolecules*; Wiley: New York, 1986.
- (4) Leckband, D.; Sheth, S.; Halperin, A. *J. Biomater. Sci., Polym. Ed.* **1999**, *10*, 1125.

- (5) Winblade, N. D.; Nikolic, I. D.; Hoffman, A. S.; Hubbell, J. A. *Biomacromolecules* **2000**, *1*, 523.
- (6) Currie, E. P. K.; Norde, W.; Cohen Stuart, M. A. *Adv. Colloid Interface Sci.* **2003**, *10*, 102–205.
- (7) Norde, W.; Gage, D. *Langmuir* **2004**, *20*, 4162.
- (8) Jeon, S. I.; Lee, J. H.; Andrade, D. J.; de Gennes, P. G. *J. Colloid Interface Sci.* **1991**, *142*, 149.
- (9) Rixman, M. A.; Dean, D.; Ortiz, C. *Langmuir* **2003**, *19*, 9357.
- (10) Curie, E. P. K.; Van der Gucht, J.; Borisov, O. V.; Cohen Stuart, M. A. *Pure Appl. Chem.* **1999**, *71*, 1227.
- (11) Efremova, N. V.; Sheh, S. R.; Leckband, D. E. *Langmuir* **2001**, *17*, 7638.
- (12) Xia, J.; Dubin, P. L.; Kokufuta, E. *Macromolecules* **1993**, *26*, 6688.
- (13) Furness, E. L.; Ross, A.; Davis, T. P.; King, G. C. *Biomaterials* **1998**, *19*, 1361.
- (14) Abbott, N. L.; Blankshtein, D.; Hatton, T. A. *Macromolecules* **1992**, *25*, 3932.
- (15) Azegami, S.; Tsuboy, A.; Izumi, T.; Hirata, M.; Dublin, P. L.; Wang, B.; Kokufuta, E. *Langmuir* **1999**, *15*, 940.
- (16) Topchieva, I. N.; Sorokina, E. M.; Efermova, N. V.; Ksenofontov, A. L.; Kurganov, B. I. *Bioconjugate Chem.* **2000**, *11*, 22.
- (17) Castelletto, V.; Krysmann, M. J.; Kellarakis, A.; Jauregi, P. *Biomacromolecules* **2007**, *8*, 2244.
- (18) Castelletto, V.; Krysmann, M. J.; Clifton, L. A.; Lambourne, J.; Noirez, L. *J. Phys. Chem. B* **2007**, *111*, 11330.
- (19) Topchieva, I. N.; Sorokina, E. M.; Kurganov, B. I.; Zhulin, V. M.; Makarova, Z. G. *Biochemistry (Moscow)* **1996**, *61*, 746.
- (20) Almeida, N. L.; Oliveira, C. L. P.; Torriani, I. L.; Loh, W. *Colloids Surf., B* **2004**, *38*, 67.
- (21) Booth, C.; Attwood, D. *Macromol. Rapid Commun.* **2000**, *21*, 501.
- (22) Booth, C.; Attwood, D.; Price, C. *Phys. Chem. Chem. Phys.* **2006**, *8*, 3612.
- (23) Carter, D. C.; Ho, J. K. *Adv. Protein Chem.* **1994**, *45*, 153.
- (24) Alexandridis, P.; Olsson, U.; Lindman, B. *Langmuir* **1997**, *13*, 23.
- (25) Kellarakis, A.; Havredaki, V.; Booth, C.; Nace, V. M. *Macromolecules* **2002**, *35*, 5591.
- (26) Hamley, I. W.; Pederson, J. S.; Booth, C.; Nace, V. M. *Langmuir* **2001**, *17*, 6386.
- (27) Yu, G.-E.; Yang, Y.-W.; Yang, Z.; Attwood, D.; Booth, C.; Nace, V. M. *Langmuir* **1996**, *12*, 3404.
- (28) Soni, S. S.; Sastry, N. V.; Patra, A. K.; Joshi, J. V.; Goyal, P. S. *J. Phys. Chem. B* **2002**, *106*, 13069.
- (29) Norman, A. I.; Ho, D. L.; Karim, A.; Amis, E. J. *J. Colloid Interface Sci.* **2005**, *205*, 155.
- (30) Nace, V. M. *J. Am. Oil Chem. Soc.* **1996**, *73*, 1.
- (31) Kellarakis, A.; Havredaki, V.; Viras, K.; Mingvanish, W.; Heatley, F.; Booth, C.; Mai, S.-M. *J. Phys. Chem. B* **2001**, *105*, 7384.
- (32) Provencher, S. W. *Makromol. Chem.* **1979**, *180*, 201.
- (33) Martinez-Landeira, P.; Ruso, J. M.; Prieto, G.; Sarmiento, F.; Jones, M. N. *Langmuir* **2002**, *18*, 3300.
- (34) Squire, P. G.; Moser, P.; O'Konski, C. T. *Biochemistry* **1968**, *7*, 4261.
- (35) Ferrer, M. L.; Duchowicz, R.; Carrasco, B.; de la Torre, J. G.; Acuna, A. U. *Biophys. J.* **2001**, *80*, 2422.
- (36) Vivares, D.; Belloni, L.; Tardieu, A.; Bonnete, F. *Eur. Phys. J. E* **2002**, *9*, 15.
- (37) Gombotz, W. R.; Guanghui, W.; Horbett, T. A.; Hoffman, A. S. *J. Biomed. Mater. Res.* **1991**, *25*, 1547.
- (38) Guinier, A. *X-ray Diffraction*; W.H. Freeman: San Francisco, 1963.
- (39) Bergstrom, M.; Pedersen, J. S. *Phys. Chem. Chem. Phys.* **1999**, *1*, 4437.
- (40) Luzzati, V.; Witz, J.; Nicolaieff, A. J. *J. Mol. Biol.* **1961**, *3*, 379.
- (41) Das, A.; Chitra, R.; Choudhury, R. R.; Ramanadham, M. *Pramana* **2004**, *63*, 363.
- (42) Filfil, R.; Chalikian, T. V. *J. Mol. Biol.* **2003**, *326*, 1271.
- (43) Filfil, R.; Chalikian, T. V. *FEBS Lett.* **2003**, *554*, 351.
- (44) Kelly, S. M.; Price, N. C. *Biochim. Biophys. Acta* **1997**, *161*, 1338.
- (45) Kelly, S. M.; Jess, T. J.; Price, N. C. *Biochim. Biophys. Acta* **2005**, *1751*, 119.
- (46) Lee, J. C.; Lee, L. L. Y. *J. Biol. Chem.* **1981**, *256*, 625.
- (47) Kim, J.-H.; Taluja, A.; Knutson, K.; Bae, Y. H. *J. Controlled Release* **2005**, *109*, 86.
- (48) Pispas, S. *J. Polym. Sci., Part A: Polym. Chem.* **2007**, *45*, 509.
- (49) Lin, V. J. C.; Koenig, J. L. *Biopolymers* **1976**, *15*, 203.
- (50) Maxfield, J.; Shepherd, I. W. *Polymer* **1975**, *16*, 505.
- (51) Brownsey, G. J.; Noel, T. R.; Parker, R.; Ring, S. G. *Biophys. J.* **2003**, *85*, 3943.

BM800046M